Available online at www.sciencedirect.com
ScienceDirect
ELSEVIER
Photonics and Nanostructures – Fundamentals and Applications 6 (2008) 38–41
PHOTONICS AND NANOSTRUCTURES
Fundamentals and Applications
www.elsevier.com/locate/photonics

Photonic crystal slotted slab waveguides

A. Di Falco *, L. O'Faolain, T.F. Krauss

School of Physics and Astronomy, North Haugh, St. Andrews, Fife KY16 9SS, UK

Received 12 June 2007; received in revised form 15 August 2007; accepted 20 August 2007
Available online 25 August 2007

Abstract

We report on the fabrication of photonic crystal waveguides in SOI that comprise an air-slot in the centre. The slot serves to confine suitably polarised optical radiation (H-polarisation) and due to its small size, provides extremely high field intensity values out with the high index material. Adding the photonic crystal environment then provides full control over the dispersive properties of this waveguide. We demonstrate the successful operation of this structure experimentally and explain its key features.

PACS : 42.70.Qs; 42.82.Et

Keywords: Photonic crystal waveguides; Integrated optics; Slotted photonic crystal waveguides; Air guiding

1. Introduction

Since the early days of integrated optics and optical communications, the advantages of confining and guiding light by total internal reflection (TIR) have been used to fabricate filters, switches and optical interconnection devices. The emerging silicon-based technology called for solutions to confine the optical beams in low index silica (or other dielectric layers) grown or deposited on high refractive index silicon. TIR could not be used so different approaches had to be developed. In 1976, Yariv and Yeh proposed Bragg reflection as a mean to achieve low loss guiding even when the guiding layer had index of refraction lower than that of the periodic layers [1], with the experimental verification being provided 1 year later [2].

A complementary approach to guiding light in low index material grown on high index substrate was firstly proposed and demonstrated by Duguay et al. [3]. In these waveguides, guiding relied on the anti-resonance of light propagating at a glancing angle to an index discontinuity.

More recently, with SOI technology providing suitable substrates for the most diverse applications, the interest in confining light in low index materials is further strengthened by applications in light-matter interaction, optical tweezing and quantum optics. Both the resonant and the antiresonant approaches have since been used to provide guiding for these purposes [4,5].

It has now even been demonstrated that TIR itself is sufficient to confine light in low index material, using a channel waveguide with a slot cut along its length, as long as the slot is of nanophotonic dimensions, i.e. of order 100 nm [6]. This geometry allows the confinement and guiding of light when it is polarised with the electrical field perpendicular to the slot, such that it strongly senses the discontinuity in the refractive index. If the air gap is narrower than the characteristic decay length of the evanescent tail of the modes inside the slot, the tails merge into a high intensity, small volume mode that propagates in air yet is guided by the semiconductor walls. Due to its peculiar properties, this approach has

* Corresponding author.
E-mail address: adfsubscription@gmail.com (A. Di Falco).

1569-4410/$ – see front matter
doi:10.1016/j.photonics.2007.08.001

attracted much attention and different configurations have been proposed, i.e. microcavities and other applications ranging from plasmonic structures to nonlinear optics [7–11].

In this paper, we show how to add versatility and functionality to the air-slot design by merging the resonant and the TIR confinement mechanisms, in particular using the inherent control over dispersive properties provided by photonic crystals (PhCs). Given that PhCs can be engineered and tailored to produce low loss waveguides and high quality microcavities [12,13], they are ideal hosts for quantum and nonlinear optics applications [14,15], as well as enhanced light-matter interaction experiments [16]. Many of these approaches are nevertheless limited by the weak overlap between the evanescent tails of the guided fields extending in air and the overlaying material.

Our idea promises to improve the efficiency of such interactions by extending the design freedom of slotted channel waveguides to an efficient management of the dispersion of air-guided modes. In the following sections we present the dispersion properties of slotted photonic crystal waveguides (SPhCWs), their fabrication procedure and their experimental characterisation.

2. Dispersion features

The properties of SPhCWs were numerically investigated using a three-dimensional plane wave expansion code [17] and tested against 3D finite difference time domain simulations (not reported here). In Fig. 1 (a) we show a schematic view of the unit cell of the proposed device. A narrow air-slot is cut into the centre of a line defect (W1) slab waveguide. The system properties are therefore defined by the refractive index of the material, the lattice constant a, the radius r of the holes and the width of the slot w. A suitable combination of these values allows us to define structures that support propagating modes which are mainly confined in air yet strongly bound to the structure. A typical mode profile is shown in Fig. 1(b) where we show the y component of the electric field in the waveguide plane (darker colours correspond to higher intensity). It is evident that most of the field is situated in air while the evanescent tails of the mode reach the high contrast periodic boundaries which therefore impress their dispersion features onto the slot mode.

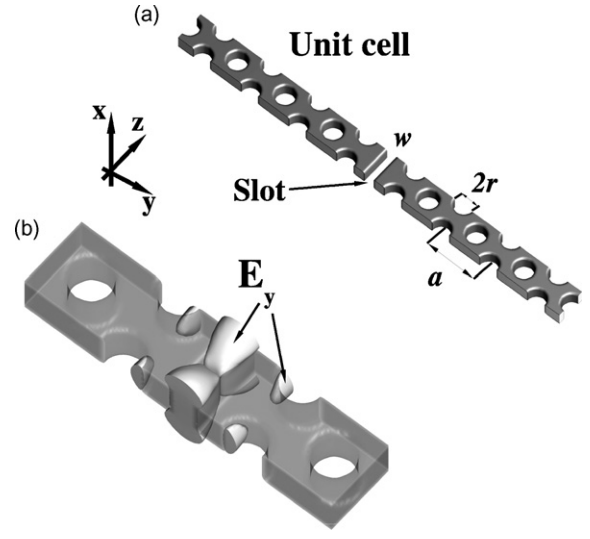

Fig. 1. (a) Pictorial view of the unit cell of the proposed device. (b) 3D isosurface of the y component of the electrical field.

The dispersive properties of the mode supported by the SPhCW can be easily understood when compared to those of a standard PhCW. The top panel of Fig. 2 shows the band diagram relative to a W1 waveguide with $r/a = 0.34$, where the shaded areas correspond to the continuum of slab modes. The light line is shown, along with the first two modes. Cutting a slot into the middle of the waveguide has two immediate effects: the even

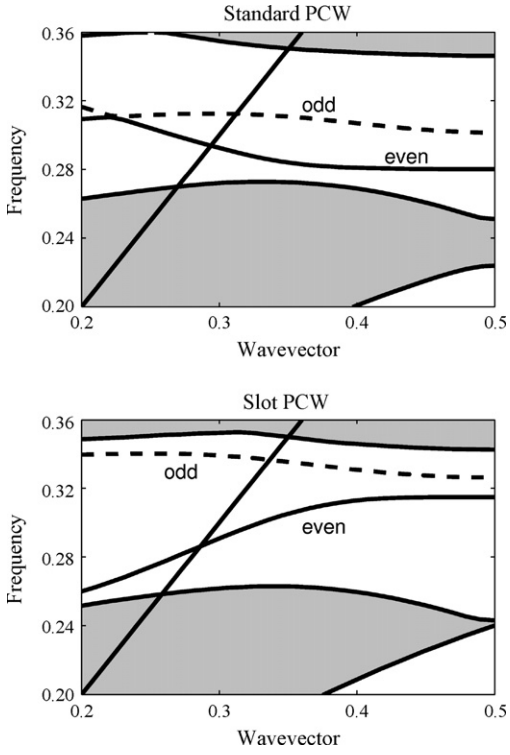

Fig. 2. (Top panel) Band diagram of a standard PhC W1 slab waveguide. (Bottom panel) Band diagram of a membrane SPhCW with $w/a = 0.31$. In both diagrams units are normalized.

mode of the W1 waveguide is suppressed due to symmetric constraint and replaced by the slot mode (please note that SPhCWs admit only even symmetry eigenmodes confined in air because the cut imposes a node in the maximum of the standard W1 modes); the odd mode is pushed towards higher frequencies because of the reduction of its filling factor (lower refractive indices blue shift the modes frequencies). Conversely, the slab mode bands are only slightly affected by the insertion of the air-slot, since their properties are predominantly determined by the uniform PC. For the refractive index of silicon at room temperature (we used $n \simeq 3.46$) and an air-slot size in the range between $0.14a$ and $0.55a$, the SPhCW structure supports a slot mode similar to the one shown in Fig. 1(b), whose dispersive features are shown in the bottom panel of Fig. 2. Please note that the slope of the dispersion curve is opposite to that of the ordinary PCW, which is typical of defect slab waveguides obtained by locally reducing the refractive index of the structure. Two of these structures were studied in Ref. [18] along with three waveguides where the defect was created by locally increasing the refractive index. It is worth noting that the type of guide discussed here completes the set of waveguides previously analyzed by Johnson et al.

3. Fabrication

The fabrication was carried out in the framework of the ePIXnet Nanostructuring Platform [19] and is similar to that reported in [20].

The devices were based on a silicon-on-insulator (SOI) wafer consisting of a 220 nm thick silicon layer, followed by a 2000 nm thick silica layer situated on a silicon carrier. The periodic patterns and the slot waveguide were defined in ZEP-520A electron beam resist using a hybrid RAITH Elphy Plus/LEO Gemini 1530 electron beam writer with 2 nm placement accuracy. Obtaining good quality sidewalls on slot-like features and holes simultaneously is non-trivial, as the etching characteristics are subtly different due to the different geometries. Some optimization of the etching regime was necessary in order to find the optimum conditions. To transfer the pattern into the silicon layer, we used reactive ion etching with a 1:1 blend of SF6 and CHF3 gases, a dc bias of 200 V and relatively low power (20 W). UV exposure and a trichloroethylene bath were used to remove the remaining photoresist. The silica cladding beneath the crystals was selectively removed with hydrofluoric acid, using windows in photoresist to protect the areas not to be etched. Fig. 3 is a scanning electron micrograph of the actual device studied here.

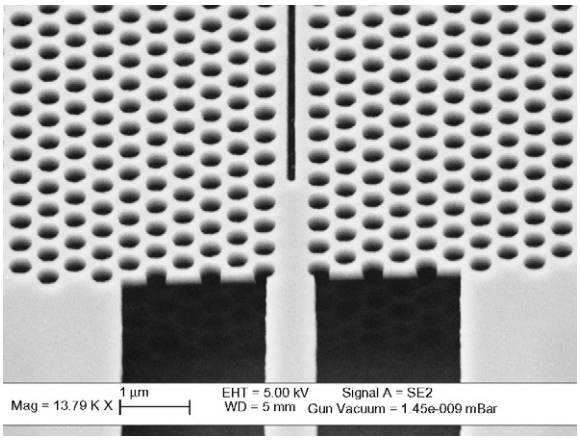

Fig. 3. SEM picture of the coupling region of the actual device.

Tapered channel waveguides were defined to launch and collect light to and from the SPhCW. The mismatch between the channel and the slot modes yields negligible coupling to the SPhCW, thus we improved the design with an additional coupling region. Standard W1 transition regions of four periods were used at the input at the output of the slot waveguides. This type of interface improves both the spatial overlap and the phase matching between the TIR mode of the channel waveguides and the peculiar slot mode of the SPhCW [21]. The period of the PhC is $a = 450$ nm; the radius of $r = 145$ nm and the slot width of $w = 140$ nm were chosen to match the transmission windows of the W1 transition region and the slot waveguide. The slot waveguide is 50 μm long.

4. Measurements

An ASE source was used to probe the transmission of the SPhCW. Light was collimated and focused onto the cleaved facet of the sample and butt-coupled to the 3 μm wide tapered channel waveguide. The signal at the output waveguide was collimated and analyzed by an OSA. The measured transmission, obtained after normalization to the source signal, is reported in arbitrary units in the top panel of Fig. 4. The slot mode cut-off falls outside the observed wavelength window (see Fig. 2), which was limited by the spectral range of the ASE source. Fringes arising from Fabry–Perot resonances caused by interface reflectivity at the slot waveguide—W1 interface are clearly visible. The bottom panel of Fig. 4 shows the same transmission in logarithmic scale along with that of standard W1 waveguide that is used as a reference. Even though the input and output interface sections are only four unit cells long at each side, their impact is clearly seen: at

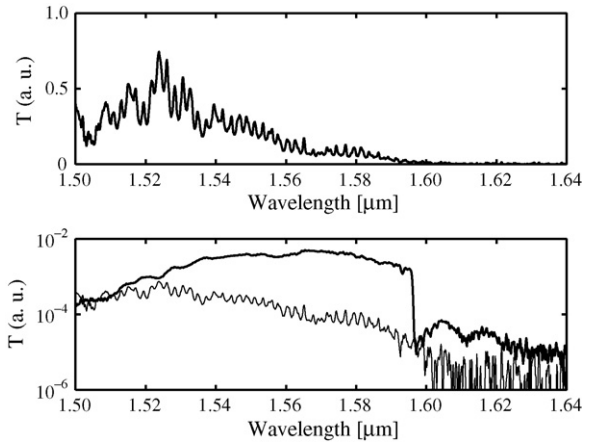

Fig. 4. (Top panel) T in arbitrary units vs. wavelength (in μm scale) of the slot waveguide. (Bottom panel) T in arbitrary units vs. wavelength (in μm scale) of the slot waveguide (thin line) and of the W1 waveguide (thick line).

longer wavelength ($\lambda > 1595$ nm, $a/\lambda = 0.282$), the transmission is limited by the cut-off of the W1 mode. Conversely, in the short wavelength region ($\lambda < 1520$ nm, $a/\lambda = 0.296$), the dispersion curve crosses the light line, so out-of-plane radiation reduces the transmission (this is a much weaker effect than the mode cut-off, however, as can also be observed by the much softer transition). The low transmission of the SPhCW in the transmission regime (1520–1595 nm), where the W1 transmission is relatively high, is due to the spatial mismatch between the respective modes (see Fig. 2). Improving this coupling efficiency is obviously the next step in developing these slotted PhC waveguides.

5. Conclusions

In conclusion, we have analyzed and experimentally verified the dispersion properties of an innovative PhC-based waveguide that combines resonant and TIR guiding mechanisms. These devices present intrinsic advantages with respect to plain slot waveguides and standard PhC waveguides, as they provide both strong overlap with air, or any functional material one may wish to place inside the air-slot, as well as controlling the dispersion and ability to provide cavity confinement. We forecast an extensive use of this approach in all applications requiring a tailored control of the dispersion of air-guided modes.

Acknowledgements

We thank Dr. D. O'Brien for useful discussions. Dr. Di Falco is supported by the Consortium of Speckled Computing (EPSRC "SpeckNet"). Dr. O'Faolain is supported by the ePIXnet Network of Excellence of the European Commission.

References

[1] A. Yariv, P. Yeh, Opt. Commun. 19 (1976) 427.
[2] A.Y. Cho, A. Yariv, P. Yeh, Appl. Phys. Lett. 30 (1977) 471.
[3] M.A. Duguay, Y. Kokubun, T.L. Koch, L. Pfeiffer, Appl. Phys. Lett. 49 (1986) 13.
[4] R.F. Cregan, B.J. Mangan, J.C. Knight, T.A. Birks, P.St.J. Russel, P.J. Roberts, D.C. Allan, Science 285 (1999) 1537.
[5] D. Yin, H. Schmidt, J.P. Barber, A.R. Hawkins, Optics Express 12 (2004) 2710.
[6] V.R. Almeida, Q. Xu, C.A. Barrios, M. Lipson, Opt. Lett. 29 (2004) 1209.
[7] Q. Xu, V.R. Almeida, R.R. Panepucci, M. Lipson, Opt. Lett. 29 (2004) 1626–1628.
[8] J.T. Robinson, C. Manolatou, L. Chen, M. Lipson, Phys. Rev. Lett. 95 (2005) 143901.
[9] H.T. Miyazaki, Y. Kurokawa, Phys. Rev. Lett. 96 (2006) 097401.
[10] T. Baehr-Jones, M. Hochberg, G. Wang, R. Lawson, Y. Liao, P.A. Sullivan, A. Dalton, A.K.-Y. Jen, A. Scherer, Optics Express 13 (2005) 5216–5226.
[11] A. Di Falco, C. Conti, G. Assanto, Opt. Lett. 31 (2006) 3146–3148.
[12] Y. Akahane, T. Asano, B.-S. Song, S. Noda, Nature 425 (2003) 944.
[13] M. Settle, M. Salib, A. Michaeli, T. Krauss, Optics Express 14 (2006) 2440.
[14] K. Hennessy, A. Badolato, M. Winger, D. Gerace, M. Atatüre, S. Gulde, S. Fält, E.L. Hu, A. Imamoğlu, Nature 445 (2007) 896.
[15] C. Conti, A. Di Falco, G. Assanto, Optics Express 12 (2004) 823.
[16] J. Bravo-Abad, M. Ibanescu, J.D. Joannopoulos, M. Soljačić, Phys. Rev. A 74 (2006) 053619.
[17] S.G. Johnson, J.D. Joannopoulos, Optics Express 8 (2001) 173, http://www.opticsexpress.org/abstract.cfm?URI=OPEX-8-3-173.
[18] S.G. Johnson, P.R. Villeneuve, S. Fan, J.D. Joannopoulos, Phys. Rev. B 62 (2000) 8212.
[19] http://www.nanophotonics.eu.
[20] L. O'Faolain, X. Yuan, D. McIntyre, S. Thoms, H. Chong, R.M. De La Rue, T.F. Krauss, Electron. Lett. 42 (2006) 1454.
[21] More details on the coupling optimizations will be reported elsewhere.